Newly born peroxisomes are a hybrid of mitochondrial and ER-derived pre-peroxisomes

Ayumu Sugiura

Monday, December 6, 2021 12:51 PM

STUDY 23

Introduction

This study investigates where peroxisomes originate.

Conclusions

Peroxisomes originate from a mixture of mitochondrial and endoplasmic reticulum vesicles that include proteins PMP70, Pex3, and Pex16.

Amendments

LETTER

doi:10.1038/nature21375

Newly born peroxisomes are a hybrid of mitochondrial and ER-derived pre-peroxisomes

Ayumu Sugiura[1], Sevan Mattie[1], Julien Prudent[1] & Heidi M. McBride[1]

Peroxisomes function together with mitochondria in a number of essential biochemical pathways, from bile acid synthesis to fatty acid oxidation[1]. Peroxisomes grow and divide from pre-existing organelles[2], but can also emerge *de novo* in the cell[3]. The physiological regulation of *de novo* peroxisome biogenesis remains unclear, and it is thought that peroxisomes emerge from the endoplasmic reticulum in both mammalian and yeast cells[4]. However, in contrast to the yeast system[5–8], a number of integral peroxisomal membrane proteins are imported into mitochondria in mammalian cells in the absence of peroxisomes, including Pex3, Pex12, Pex13, Pex14, Pex26, PMP34 and ALDP[9–15]. Overall, the mitochondrial localization of peroxisomal membrane proteins in mammalian cells has largely been considered a mis-targeting artefact in which *de novo* biogenesis occurs exclusively from endoplasmic reticulum-targeted peroxins[16]. Here, in following the generation of new peroxisomes within human patient fibroblasts lacking peroxisomes, we show that the essential import receptors Pex3 and Pex14 target mitochondria, where they are selectively released into vesicular pre-peroxisomal structures. Maturation of pre-peroxisomes containing Pex3 and Pex14 requires fusion with endoplasmic reticulum-derived vesicles carrying Pex16, thereby providing full import competence. These findings demonstrate the hybrid nature of newly born peroxisomes, expanding their functional links to mitochondria.

The initiation of *de novo* peroxisomal biogenesis requires the stepwise assembly of the peroxisomal import machinery within a nascent pre-peroxisome. In mammalian cells, this process begins with the assembly of the membrane import receptors Pex3 and Pex16, which together import peroxisomal membrane proteins bound to the cytosolic chaperone Pex19 (ref. 16). The absence of any of these proteins results in cells devoid of peroxisomal structures. These three import proteins function together to insert membrane-anchored proteins, including the machinery that imports luminal enzymes, allowing the peroxisome to mature fully. To study the earliest steps of *de novo* peroxisomal biogenesis, we used an established human fibroblast cell line lacking Pex3, obtained from a patient with Zellweger syndrome[10] ($Pex3^{mut}$; Extended Data Fig. 1a). We rescued these cells with adenoviral expression of Pex3 tagged with yellow fluorescent protein (Pex3–YFP) and monitored peroxisomal biogenesis (Fig. 1a, c). Immunofluorescence and biochemical analysis confirmed that Pex3–YFP and endogenous Pex14 first targeted the mitochondrial outer membrane in $Pex3^{mut}$ cells, adopting the same N_{in}–C_{out} orientation as when inserted into peroxisomes of control cells[9,10,17] (Fig. 1b and Extended Data Figs 1b–f, 2a). Cell-free import assays confirmed that Pex3 was inserted into mitochondria, but not into microsomes[18] (Extended Data Fig. 2b–d). We staged the biogenesis of new peroxisomes in this system, where stage 0 reflects cells with Pex3–YFP localized to mitochondria, followed by enrichment into vesicular pre-peroxisomal profiles (stage I). These structures first imported membrane proteins (PMP70) (stage II), and finally, we observed fully import-competent peroxisomes containing luminal markers such as catalase (stage III). Functional rescue was confirmed biochemically by showing that PMP70 expression, which is degraded in the absence of peroxisomes, was stabilized maximally 3–4 days after infection with adenoviral Pex3–YFP (Fig. 1d). Upon acquisition of import competence by peroxisomes, Pex3–YFP and Pex14 no longer targeted mitochondria and shifted exclusively to peroxisomes (Fig. 2a, b and Extended Data Fig. 3a, b).

We followed the formation of new peroxisomes on a cell-by-cell basis using long-term video analysis over 48 h (Supplementary Video 1). Pex3–YFP was localized exclusively in mitochondria, sometimes for days, until it transited rapidly to stage I in a stochastic manner within individual cells. In the example shown, Pex3–YFP transited to stage I and increased in intensity within pre-peroxisomal structures, and there was a simultaneous loss in mitochondrial localization over 2–4 h (Fig. 2c, magenta asterisk at 31–33 h). At a higher and faster resolution, we observed a striking enrichment of Pex3–YFP along the mitochondrial tubule, which was released within 10 s (Fig. 2d, Extended Data Fig. 2e and Supplementary Videos 2–4). Serial confocal sections confirmed that Pex3–YFP-positive structures emerging from mitochondria also carried endogenous Pex14 (Fig. 2e, Extended Data Fig. 2f and Supplementary Videos 5, 6). Mitochondrial targeting of Pex3 was required for rescue, as N-terminally tagged Pex3 failed to localize to mitochondria and did not restore peroxisomal biogenesis in $Pex3^{mut}$ cells (Extended Data Fig. 4a–c).

Although Pex3–YFP is efficiently imported into mitochondria in $Pex3^{mut}$ cells lacking peroxisomes, it is exclusively peroxisomal in nearly 99% of wild-type fibroblasts. However, we observed a small percentage of wild-type human fibroblast cells with complete Pex3–YFP staining in mitochondria (Extended Data Fig. 5a) and a marked reduction in the number of peroxisomes (Fig. 2f). The gradual loss of PMP70 in cells infected with Pex3–YFP was validated biochemically, consistent with previous evidence that Pex3–YFP expression can drive pexophagy[19] (Extended Data Fig. 5b). Video analysis allowed us to visualize cells in which Pex3–YFP was initially targeted to peroxisomes; however, the peroxisomal Pex3–YFP signal was depleted over a few hours (Extended Data Fig. 5c and Supplementary Video 7). Following this, Pex3–YFP slowly accumulated in mitochondria, remaining there for the remainder of the experiment. This finding reveals an unexpected ability of wild-type cells to rapidly retarget Pex3 to mitochondria under conditions of global pexophagy.

We confirmed that stage I vesicular profiles carrying Pex3–YFP or Pex14 did not target the lysosomal-degradation pathway[20], as vesicles did not colocalize with the lysosome-associated membrane protein Lamp1b, and the inhibitor of lysosomal acidification, bafilomycin A had no impact on *de novo* peroxisomal biogenesis or Pex3 turnover (Fig. 3a, b and Extended Data Fig. 6a, b). By contrast, inhibition of proteasome degradation by MG132 led to accumulation of Pex3–YFP within mitochondria and blocked *de novo* peroxisome synthesis (Fig. 3a, b). Addition of cycloheximide to arrest protein synthesis led to the loss of Pex3–YFP in both control and $Pex3^{mut}$ cells within 3 h (Extended Data Fig. 7a, b). Immunoprecipitation of Pex3–YFP in the

[1]Montreal Neurological Institute, McGill University, 3801 University Ave, Montreal, Quebec, H3A 2B4, Canada.

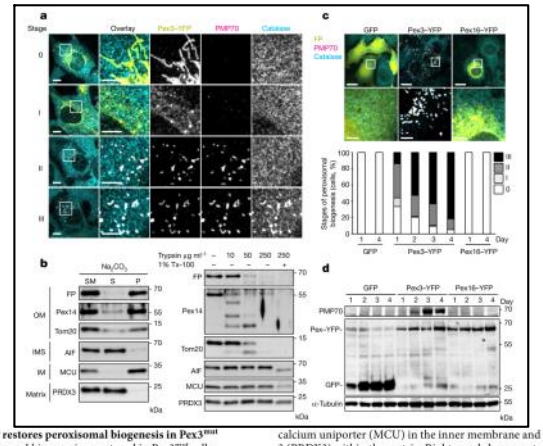

Figure 1 | Pex3–YFP restores peroxisomal biogenesis in Pex3^{mut} fibroblasts. a, Peroxisomal biogenesis was staged in Pex3^{mut} cells infected with Ad-Pex3–YFP using anti-PMP70 and catalase antibodies. Representatives of 225 captured cells are shown. Scale bars: first column, 10 µm; other columns, 5 µm. **b**, Pex3–YFP and endogenous Pex14 were isolated within the membrane fraction of isolated mitochondria (2.3K pellet) of Pex3^{mut} cells 1 day after infection with Pex3–YFP (left). S, soluble fraction; P, membrane fraction; OM, outer membrane; IMS, intermembrane space; IM, inner membrane; SM, starting material; FP, anti-GFP antibodies to detect Pex3–YFP. Internal controls were probed as indicated, where Translocator of outer membrane (Tom20) is in the OMM, apoptosis-inducing factor (AIF) within the IMS, mitochondrial calcium uniporter (MCU) in the inner membrane and peroxiredoxin 3 (PRDX3) within the matrix. Right panel shows protease accessibility of each protein, as indicated. **c**, Rescue of Pex3^{mut} cells infected with indicated adenoviruses, with representatives of counted cells from day 4 shown. The graph represents the percentage of cells at each stage of *de novo* synthesis defined in **a**. Data from three biological replicates. Number of cells counted in each experiment: GFP: day 1 (51, 56, 51), day 4 (53, 57, 55); Pex3–YFP: day 1 (83, 62, 90), day 2 (114, 94, 88), day 3 (68, 57, 59), day 4 (73, 58, 69); Pex16–YFP: day 1 (52, 60, 71), day 4 (51, 63, 60). Scale bars: top, 20 µm; bottom, 5 µm. **d**, Stabilization of PMP70 within Pex3^{mut} cells rescued with Ad-Pex3–YFP. Expression of tagged and endogenous proteins is revealed by western blot, as indicated.

presence of MG132 showed an accumulation of ubiquitinated proteins, confirming that the rapid turnover of Pex3–YFP occurs through the ubiquitin–proteasome system[19] (Extended Data Fig. 7c, d).

Although vesicle release often requires dynamic assembly of actin filaments, inhibition of actin polymerization by cytochalasin D did not alter peroxisomal biogenesis (Fig. 3b and Extended Data Fig. 6b). However, addition of nocodazole inhibited the exit of Pex3–YFP from mitochondria, again delaying peroxisomal biogenesis (Fig. 3b). This inhibition was due to the activation of Rho kinase by nocodazole[21], as cells co-treated with the Rho kinase inhibitor Y-27632 did not show inhibition (Extended Data Fig. 6c). These data show that Pex3–YFP must exit mitochondria to mediate peroxisomal biogenesis.

We next tested candidate machinery that may be required for the exit of Pex3–YFP from mitochondria, including the peroxisomal and mitochondrial division GTPase Drp1 (ref. 22), the retromer component requisite for transport of mitochondrial-derived vesicle to peroxisomes Vps35 (ref. 23) and the peroxisomal import chaperone for membrane proteins Pex19 (ref. 24–26; Extended Data Fig. 8a–c). Loss of these factors did not alter the targeting or exit of Pex3–YFP from mitochondria, indicating that novel, unidentified machinery is responsible for this process.

Ultrastructural analysis of Pex3^{mut} fibroblasts revealed mitochondria with abundant cristae, but we observed unusual electroluscent structures along the sides of many mitochondria (Fig. 3c). These structures increased in size upon rescue with Pex3–YFP, with diameters beyond 250 nm. Constrictions were observed at the necks of these structures, consistent with the pinching of membrane required for vesicle release (Fig. 3c, arrowhead). Immunogold staining revealed a striking accumulation of Pex3–YFP on these structures (Fig. 3d), consistent with confocal evidence of Pex3 enrichment within vesicular profiles released from mitochondria (Supplementary Videos 2–4).

The most compelling evidence that peroxisomes are derived from the endoplasmic reticulum (ER) in mammalian cells is that Pex16 targets the ER in cells lacking peroxisomes[12,15,27]. We therefore used a fibroblast cell line lacking Pex16 (Pex16^{mut}) from a patient with Zellweger syndrome[25,27] (Extended Data Fig. 1a). Ectopically expressed Pex16–YFP targeted the ER and rescued the formation of mature peroxisomes by 4 days (Fig. 4a and Extended Data Fig. 9a, b). As in Pex3^{mut} cells, endogenous Pex14 targeted the mitochondrial outer membrane in Pex16^{mut} fibroblasts (Extended Data Fig. 1b–f). Confocal imaging of Pex16–YFP rescue showed accumulation of Pex16–YFP within vesicular profiles at early time points. Pex14 was initially absent from Pex16 vesicles (Fig. 4b). We next observed a second stage during which Pex14 was enriched within Pex16-positive structures, which were in very close contact with mitochondria (Fig. 4b, Extended Data Fig. 9c and Supplementary Video 8). Unlike Pex3–YFP, the release of Pex16–YFP from the ER was unaffected by treatment with nocodazole (Extended Data Fig. 9d). Immunogold staining of Pex16–YFP in Pex16^{mut} cells confirmed that Pex16 was localized to the ER, and also showed labelling on vesicular structures throughout the cytoplasm and in approximately 100-nm structures in direct contact with mitochondria (Fig. 4c). These data confirm the presence of ER-derived Pex16 in pre-peroxisomal vesicular profiles.

Figure 1

These data are in cells that lack the Pex3 peroxisome protein.

[1A] This data shows the various stages of peroxisome formation, Pex3 -YFP being a marker for peroxisomes, PMP70 being a marker for mature peroxisomes, and Catalase is a marker of mature peroxisomes (an enzyme that removes reactive oxygen species). **Primary Results:** Pex3 being mitochondrial associated in stage 0, then associating more with PMP70 (a protein associated with maturing/mature peroxisomes) and catalase (an enzyme associated with mature peroxisomes) in later stages.

[1C] Pex3 transfection (in Pex3 deficient cells) leads to generation of peroxisomes (co - localized with PMP70 and Catalase), but Pex16 transfection had no effect.

[1D] PMP70 is stabilized when peroxisomes are present, so the researchers infected the cells with an empty gene (GFP), Pex3, or Pex16 (both peroxisome associated genes/proteins) and looked at the stabilization of PMP70. **Primary Results:** PMP70 is only stabilized/present when Pex3 is expressed.

Take Away: Pex3 is necessary for the generation and maturation of peroxisomes and Pex3 is mitochondria associated.

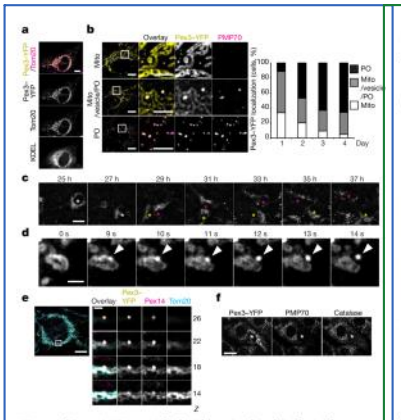

Figure 2 | Pex3–YFP is enriched within mitochondria-derived pre-peroxisomal structures. a, Pex3^{mut} cells were infected with Ad-Pex3–YFP and stained with anti-Tom20 (mitochondria) and anti-KDEL (ER) antibodies. A representative of 122 captured cells is presented. Scale bar, 10 μm. **b**, Quantification of Pex3–YFP localization during the rescue. Left, representative images. Graph includes data from three biological replicates. Number of cells counted: day 1 (83, 62, 90), day 2 (114, 94, 88), day 3 (68, 57, 59), day 4 (73, 58, 69). Scale bars: left column, 10 μm; other columns, 5 μm. Mito, mitochondria; PO, peroxisome. **c**, Pex3^{mut} cells rescued with Ad-Pex3–YFP were visualized over 48 h. A representative of 68 movies is shown. Magenta and yellow asterisks indicate cells in which Pex3–YFP translocated from mitochondria to peroxisomes or remained in mitochondria, respectively. Time after infection is shown. Scale bar: 20 μm. **d**, Pex3–YFP-expressing pre-peroxisomal structures are released from mitochondria. Images captured from Pex3^{mut} cells infected with Ad-Pex3–YFP. A representative of 30 movies is shown. Arrowheads, Pex3–YFP-enriched structure. Scale bar: 2 μm. **e**, Z series of Pex3^{mut} cells infected with Ad-Pex3–YFP, immunostained with anti-Pex14 and anti-Tom20 antibodies. The numbers represent images at indicated Z. A representative of 60 captured cells is shown. Scale bars: left panel, 10 μm; other panels, 2 μm. **f**, Control human fibroblasts reveal mitochondrial targeting of Ad-Pex3–YFP in cells devoid of peroxisomes (asterisk). Representatives of 230 captured cells are shown. Scale bar: 20 μm.

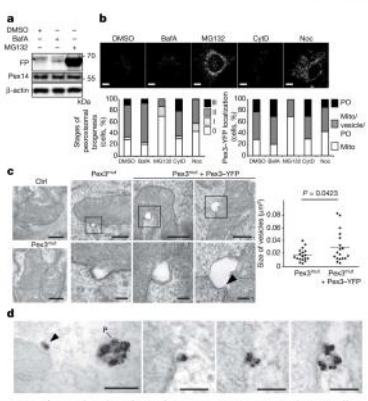

Figure 3 | Mitochondria-derived pre-peroxisomes are mechanistically and structurally distinct from mitochondrial division or vesicle formation. Ten hours after infection, Pex3^{mut} cells were treated with the indicated drugs for 14 h. **a**, Pex3–YFP levels were unaltered in the presence of bafilomycin A (BafA), but increased in the presence of the proteasome inhibitor MG132. Asterisk, nonspecific band; antibodies indicated. **b**, Representative images of rescue in the presence of the indicated drugs, quantified by the stages of *de novo* synthesis (left) or localization of Pex3–YFP (right). Data taken from three biological replicates. Cells counted: DMSO (59, 50, 57), BafA (56, 54, 52), MG132 (51, 52, 54), cytochalasin D (CytD) (52, 54, 52), nocodazole (Noc) (57, 54, 54). Scale bars, 10 μm. **c**, Ultrastructural analysis of mitochondria in control (Ctrl), Pex3^{mut}, and Pex3^{mut} cells rescued with Ad-Pex3–YFP. Boxed areas are magnified in lower panels. Representatives are shown from 21 cells (control), 88 cells (Pex3^{mut}) and 53 cells (Pex3^{mut} + Pex3–YFP. Arrowhead shows constricted neck of pre-peroxisome. Scale bars: top, 500 nm; bottom, 100 nm. Dot plot represents sizes of emerging vesicles ($n = 18$ each). Mean is shown with P value calculated from unpaired Student's t-test. **d**, Left, Pex3–YFP in Pex3^{mut} cells labelled with immunogold reveals enrichment within structures budding from mitochondria (arrowheads) and in mature peroxisome (P). Scale bars, 200 nm. Bottom, different stages of nascent peroxisome maturation. Representatives of 105 captured images are presented. Scale bars, 100 nm.

To test directly whether Pex16 and Pex3 must localize to distinct organelles for peroxisomal biogenesis, we transfected Pex16 tagged with monomeric red fluorescent protein (Pex16–mRFP) into Pex3^{mut} cells during adenovirus-driven Pex3–YFP rescue. As previously observed, overexpression of Pex16 led to the re-routeing of Pex3–YFP to the ER[15,18] (Extended Data Fig. 10a, bottom cell). Both proteins were enriched together within ER-derived vesicular structures, defined as stage I. However, re-routeing Pex3–YFP to the ER markedly reduced the transition to import-competent peroxisomes (Extended Data Fig. 10b). These findings indicate that Pex3 must come from the mitochondria to efficiently generate functional peroxisomes, and that ER-derived pre-peroxisomal vesicles carrying Pex16 and Pex3 are not sufficient to initiate the rapid import of peroxisomal membrane proteins. Last, we performed whole-cell fusion experiments to directly visualize fusion events between ER-derived Pex16 structures and mitochondria-derived Pex3 vesicles (Fig. 4d and Extended Data Fig. 10c). Three hours after cell fusion, Pex16–mRFP-positive vesicles were transported to Pex3–YFP-enriched regions along the mitochondrial tubules (Fig. 4d, arrowheads, Extended Data Fig. 10d, circles and Supplementary Videos 9, 10). The fluorescent signals of Pex3–YFP and Pex16–mRFP coalesced within 30 s, followed by the release of a single structure from mitochondria, consistent with a dual origin of import-competent peroxisomes.

Our findings demonstrate an essential role for mitochondria in the *de novo* generation of peroxisomes in mammalian cells. This is consistent with emerging evolutionary theories positing that peroxisomes evolved after mitochondrial ancestors entered the archaebacterial host, contributing to the rise of the endomembrane system within eukaryotic cells[28,29]. Our data show remarkable segregation of the core peroxisomal import machinery between two distinct organelles; the ER and mitochondria. This segregation would ensure that import competence is acquired only upon fusion between pre-peroxisomes (see model in Extended Data Fig. 10e). Once peroxisomes are formed, they proliferate primarily through growth and division cycles. The clearance of peroxisomes by pexophagy leads to the mitochondrial import of Pex3, allowing new cycles of *de novo* peroxisomal biogenesis

Figure 2

This data is in Pex3 deficient cells (again), except final panel.

[2B] The researchers are transfecting the cells with Pex3 (a marker of peroxisomes) and watching, over 4 days, the localization of Pex3 and PMP70 (a marker of mature peroxisomes) to define the distribution of Pex3 across time (is it in mitochondria? Mitochondondrial vesicles? Or in independent peroxisomes?) **Primary Results:** Pex3 begins in the mitochondrion, then gets sequestered into vesicles, then found co-localized with PMP70 in individuals peroxisomes.

[2D] These are timed images following the progression of a peroxisome (technically, a pre-peroxisome) being released from mitochondria.

[2E] This is a stack of images showing the depth of the cell, showing co-localization of Pex3, Pex14 (peroxisome markers), and TOM20 (mitochondrial marker). As the Z images increase, the depth of imaging changes - this allows us to see the co-localization of two markers independent of the third, then introduce the third as the microscope changes its depth of view. **Primary Results:** Pex3 and Pex14 co-localize, and then both co-localize with TOM20.

Take Away: Pex3 originates from the mitochondrion and pinches off to interact with PMP70 to generate peroxisomes.

Figure 3

[3A] The researchers have exposed the cells to various inhibitors - BafA inhibits autophagy, and MG-132 inhibits proteasomal degradation (two mechanisms of protein destruction) or nothing (DMSO), and are measuring the amount of peroxisomes (FP). **Primary Result:** Autophagy inhibition has no effect on peroxisome degradation, but the loss of proteasomal degradation leads to an accumulation of peroxisomes.

[3B] To investigate this further, they looked at the same inhibitors, but instead of measuring protein amount, they observed the changes in the cells under the microscope. What stages of peroxisome formation (0-3) are more pronounced with each inhibitor (Noc is a microtubule inhibitor). **Primary Result:** Proteasomal inhibition leads to peroxisome formation stuck in stage 0, inhibiting the formation of new peroxisomes.

[3D] Under light microscopy, the researchers show the accumulation of Pex3 in mitochondria until it accumulates enough to be released as a peroxisome.

Take Away: Peroxisomes are degraded by the proteasome and the loss of proteasomal degradation leads to the peroxisomal formation to stall in stage 0 (accumulating Pex3). Under normal circumstances, Pex3 accumulates in mitochondria in a vesicle, which is eventually released full of Pex3 protein.

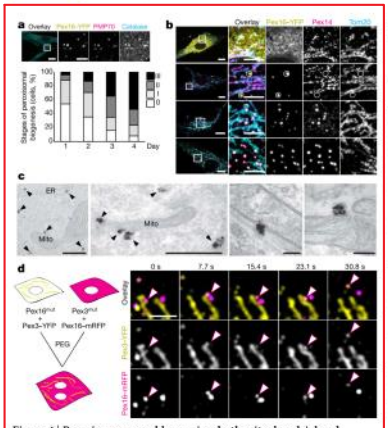

Figure 4 | Peroxisome assembly requires both mitochondrial and ER-derived pre-peroxisomes. a, Top, stages of Ad-Pex16–YFP rescue of Pex16^{mut} cells, with representative images shown. Quantification calculated from three biological replicates. Cells per experiment: day 1 (65, 44, 50), day 2 (36, 56, 48), day 3 (49, 51, 43), day 4 (40, 59, 52). Scale bars: left, 10 μm; right, 5 μm. **b**, Pex16^{mut} cells expressing Pex16–YFP were stained with anti-Pex14 and anti-Tom20 antibodies. Representatives of 31 cells are shown. Circles highlight Pex16 structures lacking Pex14. Scale bars: left column, 10 μm; right columns, 5 μm. **c**, Pex16^{mut} cells infected with Ad-Pex16–YFP were labelled with immunogold. Representatives of 27 captured images are presented. Arrowheads indicate Pex16-positive vesicle structures. Scale bars: left two panels, 500 nm; right two panels, 100 nm. **d**, Schematic on the left illustrates the steps to generate the fused heterokaryons between Pex16 and Pex3 mutant cells used to directly follow Pex16 delivery to mitochondria. Pex16^{mut} cells expressing Pex3–YFP and Pex3^{mut} cells expressing Pex16–mRFP were fused and analysed by video over 3 h. Arrowheads indicate Pex16 structures that fuse with Pex3-positive enrichments along mitochondria, which are subsequently released. Scale bar, 4 μm. PEG, polyethylene glycol.

to occur. Together, our findings provide a new mechanistic framework with which to understand the signals that regulate *de novo* peroxisomal biogenesis and its physiological importance in complex mammalian systems.

Online Content Methods, along with any additional Extended Data display items and Source Data, are available in the online version of the paper; references unique to these sections appear only in the online paper.

Received 20 April 2016; accepted 10 January 2017.
Published online 1 February 2017.

1. Mohanty, A. & McBride, H. M. Emerging roles of mitochondria in the evolution, biogenesis, and function of peroxisomes. *Front. Physiol.* **4,** 268 (2013).
2. Lazarow, P. B. & Fujiki, Y. Biogenesis of peroxisomes. *Annu. Rev. Cell Biol.* **1,** 489–530 (1985).
3. Agrawal, G. & Subramani, S. De novo peroxisome biogenesis: Evolving concepts and conundrums. *Biochim. Biophys. Acta* **1863,** 892–901 (2016).
4. Smith, J. J. & Aitchison, J. D. Peroxisomes take shape. *Nat. Rev. Mol. Cell Biol.* **14,** 803–817 (2013).
5. Titorenko, V. I., Chan, H. & Rachubinski, R. A. Fusion of small peroxisomal vesicles *in vitro* reconstructs an early step in the *in vivo* multistep peroxisome assembly pathway of *Yarrowia lipolytica*. *J. Cell Biol.* **148,** 29–44 (2000).
6. van der Zand, A., Braakman, I. & Tabak, H. F. Peroxisomal membrane proteins insert into the endoplasmic reticulum. *Mol. Biol. Cell* **21,** 2057–2065 (2010).
7. Lam, S. K., Yoda, N. & Schekman, R. A vesicle carrier that mediates peroxisome protein traffic from the endoplasmic reticulum. *Proc. Natl Acad. Sci. USA* **107,** 21523–21528 (2010).
8. Agrawal, G., Joshi, S. & Subramani, S. Cell-free sorting of peroxisomal membrane proteins from the endoplasmic reticulum. *Proc. Natl Acad. Sci. USA* **108,** 9113–9118 (2011).
9. Sacksteder, K. A. *et al.* PEX19 binds multiple peroxisomal membrane proteins, is predominantly cytoplasmic, and is required for peroxisome membrane synthesis. *J. Cell Biol.* **148,** 931–944 (2000).
10. South, S. T., Sacksteder, K. A., Li, X., Liu, Y. & Gould, S. J. Inhibitors of COPI and COPII do not block PEX3-mediated peroxisome synthesis. *J. Cell Biol.* **149,** 1345–1360 (2000).
11. Muntau, A. C., Mayerhofer, P. U., Paton, B. C., Kammerer, S. & Roscher, A. A. Defective peroxisome membrane synthesis due to mutations in human PEX3 causes Zellweger syndrome, complementation group G. *Am. J. Hum. Genet.* **67,** 967–975 (2000).
12. Kim, P. K., Mullen, R. T., Schumann, U. & Lippincott-Schwartz, J. The origin and maintenance of mammalian peroxisomes involves a de novo PEX16-dependent pathway from the ER. *J. Cell Biol.* **173,** 521–532 (2006).
13. Halbach, A. *et al.* Targeting of the tail-anchored peroxisomal membrane proteins PEX26 and PEX15 occurs through C-terminal PEX19-binding sites. *J. Cell Sci.* **119,** 2508–2517 (2006).
14. Toro, A. A. *et al.* Pex3p-dependent peroxisomal biogenesis initiates in the endoplasmic reticulum of human fibroblasts. *J. Cell. Biochem.* **107,** 1083–1096 (2009).
15. Aranovich, A., Hua, R., Rutenberg, A. D. & Kim, P. K. PEX16 contributes to peroxisome maintenance by constantly trafficking PEX3 via the ER. *J. Cell Sci.* **127,** 3675–3686 (2014).
16. Kim, P. K. & Hettema, E. H. Multiple pathways for protein transport to peroxisomes. *J. Mol. Biol.* **427** (6 Pt A), 1176–1190 (2015).
17. Schmidt, F. *et al.* The role of conserved PEX3 regions in PEX19-binding and peroxisome biogenesis. *Traffic* **13,** 1244–1260 (2012).
18. Mayerhofer, P. U., Bano-Polo, M., Mingarro, I. & Johnson, A. E. Human peroxin PEX3 is co-translationally integrated into the ER and exits the ER in budding vesicles. *Traffic* **17,** 117–130 (2016).
19. Yamashita, S., Abe, K., Tatemichi, Y. & Fujiki, Y. The membrane peroxin PEX3 induces peroxisome-ubiquitination-linked pexophagy. *Autophagy* **10,** 1549–1564 (2014).
20. Soubannier, V. *et al.* A vesicular transport pathway shuttles cargo from mitochondria to lysosomes. *Curr. Biol.* **22,** 135–141 (2012).
21. Chang, Y. C., Nalbant, P., Birkenfeld, J., Chang, Z. F. & Bokoch, G. M. GEF-H1 couples nocodazole-induced microtubule disassembly to cell contractility via RhoA. *Mol. Biol. Cell* **19,** 2147–2153 (2008).
22. Schrader, M., Bonekamp, N. A. & Islinger, M. Fission and proliferation of peroxisomes. *Biochim. Biophys. Acta* **1822,** 1343–1357 (2012).
23. Braschi, E. *et al.* Vps35 mediates vesicle transport between the mitochondria and peroxisomes. *Curr. Biol.* **20,** 1310–1315 (2010).
24. Fang, Y., Morrell, J. C., Jones, J. M. & Gould, S. J. PEX3 functions as a PEX19 docking factor in the import of class I peroxisomal membrane proteins. *J. Cell Biol.* **164,** 863–875 (2004).
25. Matsuzaki, T. & Fujiki, Y. The peroxisomal membrane protein import receptor Pex3p is directly transported to peroxisomes by a novel Pex19p- and Pex16p-dependent pathway. *J. Cell Biol.* **183,** 1275–1286 (2008).
26. Neufeld, C. *et al.* Structural basis for competitive interactions of Pex14 with the import receptors Pex5 and Pex19. *EMBO J.* **28,** 745–754 (2009).
27. South, S. T. & Gould, S. J. Peroxisome synthesis in the absence of preexisting peroxisomes. *J. Cell Biol.* **144,** 255–266 (1999).
28. Bolte, K., Rensing, S. A. & Maier, U. G. The evolution of eukaryotic cells from the perspective of peroxisomes: phylogenetic analyses of peroxisomal beta-oxidation enzymes support mitochondria-first models of eukaryotic cell evolution. *BioEssays* **37,** 195–203 (2015).
29. Gould, S. B., Garg, S. G. & Martin, W. F. Bacterial vesicle secretion and the evolutionary origin of the eukaryotic endomembrane system. *Trends Microbiol.* **24,** 525–534 (2016).

Supplementary Information is available in the online version of the paper.

Acknowledgements This work was supported by CIHR grant MOP#133549 and a Canada Research Chair to H.M.M. A.S. was supported by a JSPS Postdoctoral Fellowship for Research Abroad. S.M. through a Quebec FRQS Studentship, and J.P. by a CIHR Postdoctoral Fellowship (MFE-140925). The authors thank P. Kim for critical reagents and advice, and M. Nguyen for help with import assays.

Author Contributions H.M.M. and A.S. designed the experiments and wrote the manuscript, S.M. performed the EM analysis, J.P. contributed to the experimental design and to the quantitative microscopic analysis, and A.S. performed all experiments.

Author Information Reprints and permissions information is available at www.nature.com/reprints. The authors declare no competing financial interests. Readers are welcome to comment on the online version of the paper. Correspondence and requests for materials should be addressed to H.M.M. (heidi.mcbride@mcgill.ca).

Figure 4

These cells are deficient in Pex16.

[4B] The researchers are taking images of 4 cells and looking at the co-localization of Pex16 (a peroxisome marker that is associated with endoplasmic reticulum), Pex14 (a peroxisome marker associated with mitochondria), and Tom20 (a mitochondrial marker). **Primary Results:** In some images, there is an overlap of Pex14 and Pex16, indicating mature peroxisomes, but there are also Pex14 and Tom20 overlap that do not co-localize with Pex16, implicating Pex14 as a mitochondrial associated peroxisome marker while Pex16 is not.

[4C] Light microscopy images show Pex16 accumulated structures independent of mitochondria, around ER (according to the researchers - I think it would be better to define the mitochondria, because the proximity is extremely close).

[4D] The researchers transfected a yellow fluorescing Pex3 and a red/pink fluorescing Pex16 and wanted to track their movement over time. It is assumed that the yellow Pex3 is localized in mitochondria. **Primary Result:** Pex16 is independent of the mitochondria associated Pex3 (0-15.4sec) until it approaches and fuses with the mitochondria (likely in a vesicle), mixing with Pex3 (23.1sec), before being released from the mitochondrion with a mixture of both Pex16 and Pex3 (30.8sec).

Take Away: Pex16 pre-peroxisomes merges, temporarily, with mitochondrial Pex3 mitochondria associated pre-peroxisomes, and then separates into, presumably, mature peroxisomes containing both Pex16 and Pex3 proteins.

METHODS

Materials. Polybrene, bafilomycin A, nocodazole and cyclohexamide were purchased from Sigma. CLAAAP (protease inhibitor cocktail) and PhosStop (phosphatase inhibitor) were purchased from Roche. Cytochalasin D was obtained from Fluka.

Each antibody was obtained as follows: α-tubulin (B-5-1-2, Santa Cruz Biotechnology), AIF (sc-13116, Santa Cruz Biotechnology), β-actin (AC-74, Sigma), calnexin (ADI-SPA-860, ENZO Life Sciences), catalase (219010, Millipore), Drp1 (611113, BD Transduction Laboratories), FLAG (M2, Sigma), GFP for western blots (JL-8, Clontech), GFP (anti FP) for electron microscopy and immunoprecipitation (A6455, Life Technology), IP_3R1 (8568, Cell Signalling), KDEL (ab50601, Abcam), Lamp1b (H5G11, Santa Cruz Biotechnology), MCU (HPA016480, Sigma), MUL1 (HPA017681, Sigma), myc (4A6, Upstate), PEX14 (ABC142, Millipore), PMP70 (sab4200181, Sigma), PRDX3 (ref. 30), Tom20 (FL-145, Santa Cruz Biotechnology), ubiquitin (P4D1-A11, Millipore), VDAC1 (20B12AF2, Abcam), Vps35 (2D3, Novus).

Cell culture and transfection. The human peroxisomal biogenesis-deficient fibroblast cell line PBD400-T1 was derived from a patient with Zellweger syndrome carrying a single nucleotide insertion (c542insT) leading to a premature stop codon in the core peroxin gene *PEX3* (called $Pex3^{mut}$), a gift from P. Kim (Univ. Toronto, Canada). $Pex16^{mut}$ cells were derived from a patient with Zellweger syndrome carrying a terminating mutation in *PEX16*, R176ter (GM06231 cells, Coriell Institute, called $Pex16^{mut}$), which were immortalized as described in ref. 31. Control human fibroblasts (cell line MCH64) were obtained from Montreal Children's Hospital. The cell lines were validated using qRT–PCR to confirm the loss of Pex3 or Pex16 (data shown in Extended Data Fig. 1a).

Cells were maintained in DMEM (GIBCO) supplied with 10% fetal bovine serum (Wisent Bio Products) and non-essential amino acids (GIBCO) in 5.0% CO_2 at 37 °C. Cells were tested for mycoplasma contamination using MycoAlert Mycoplasma Detection kit (Lonza). Transfection with plasmid DNA or siRNA was performed with Lipofectamine 3000, Nucleofector (Lonza) or RNAiMAX (Invitrogen) following the manufacturer's instructions.

Addition of drugs to monitor peroxisome biogenesis was performed using the following conditions: 0.02% DMSO, 20 nM bafilomycin A, 2 μM MG132, 1 μM cytochalasin D or 1.5 μM nocodazole for 14 h.

siRNA. Series of ON-TARGETplus siRNAs were purchased from Dharmacon. Non-targeting control pool (D-001810-10), targeted sequences are as follows: ON-TARGETplus DNML1 siRNA smart pool (J-012092-09 – 12, GUUAACCCGUGGAUGAUAA, CGUAAAAGGUUGCCUGUUA, CAUCAGAGAUGUUUACCA, GGAGCCAGCUAGAUAUUAA), ON-TARGETplus smart pool siVps35 (GAACAUAUUGCUACCAGUA, GAAAGAGCAUGAGUUGUUA, GUUGUAAACUGUAGGGAUG, GAACAAAUUUGGUGCGCCU), ON-TARGETplus siPEX19 (J-012594-05, J-012594-06, J-012594-07, J-012594-08)

Adenovirus infection. C-terminal YFP-fused Pex3 (UniProtKB: P56589) and Pex16 (UniprtoKB: Q9Y5Y5) (obtained from P. Kim[12], GFP tag switched for YFP using standard procedures) were subcloned into D2-MCS viral vector (BioVector) under the control of a CMV promoter. Ad-GFP, Ad-Pex3–YFP and Ad-Pex16–YFP were used to infect cells at 50, 500 and 200 pfu per cell, respectively, in the presence of 4 μg/ml polybrene. Medium was replaced 1 day after infection.

Immunofluorescence staining. Cells were fixed with pre-warmed 5% PFA that was added directly to cells just after removing the culture medium without PBS wash. After incubation at 37 °C for 15 min, PFA was quenched with 50 mM NH_4Cl/PBS for 10 min at room temperature. Cells were permeabilized with 0.1% Triton X-100/PBS (v/v) for 10 min at room temperature and blocked with 5% FBS/PBS for 10 min at room temperature. Cells were incubated with appropriate primary antibodies for 2 h. After the wash with PBS, cells were incubated with secondary antibodies for 1 h. Cells were observed with spinning confocal microscopy (Olympus IX81 with Andor/Yokogawa spinning disk system (CSU-X), sCMOS camera and 100× or 60× objective lenses (NA1.4)). For quantification analysis, more than 30 cells in each condition were randomly chosen and counted based on the definitions on main figures (stages of *de novo* synthesis: Fig. 1a; localization of Pex3–YFP: Fig. 2b, left).

Live cell imaging. Cells plated in a glass-bottom cell culture dish (MatTek) were infected with adenoviruses. Twenty-four hours after infection, cells were incubated with 100 nM MitoTracker Deep Red FM (Molecular Probes) for 20 min at 37 °C. Cells were washed in DMEM and observed in DMEM containing no phenol red (31053028, GIBCO) supplied with 10% FBS and 2 mM L-glutamine, NEAA and 10 mM HEPES pH 7.4 using a spinning disk confocal microscope (described above) with a 100× objective and EMCCD camera. For long-term imaging (40–48 h), infected cells in phenol red-free medium were monitored with Viva View FL Incubator microscope fitted with a 40× objective (Olympus) beginning 24 h after initial infection.

PEG cell fusion. $Pex3^{mut}$ and $Pex16^{mut}$ cells were transfected with Pex16–mRFP and infected with Ad-Pex3–YFP. Sixteen hours later, cells were trypsinized and co-plated into a glass bottom cell culture dish (MatTek). One day after that, cells were fused with 50% (w/v) PEG (Fluka, MW: 1,500 Da) in MEM (Invitrogen) containing medium for 1 min. After extensive washing (5×) with DMEM, cells were monitored with the spinning disk confocal microscope beginning 1 h after whole-cell fusion[32].

Transmission electron microscopy. Cells prepared for electron microscopy were infected as indicated for 1 day before processing to capture the early events in peroxisomal biogenesis. As previously described[33], cells were fixed with 5% PFA and 1.6% glutaraldehyde (GA) in 0.1 M sodium cacodylate buffer (pH 7.4) for 10 min at room temperature, then further fixed at 4 °C in the same buffer overnight. After washing with 0.1 M cacodylate buffer, cells were fixed with 1% osmium tetroxide for 60 min at 4 °C. Cells were washed with water, stained with saturated aqueous uranyl acetate for 45 min at room temperature, and then gradually dehydrated with a series of increasing concentrations of ethanol (70–100%). After dehydrating with 100% acetone, cells were gradually embedded in Spurr's resin, and polymerized for 48 h at 60 °C. Samples were sectioned to a 100-nm thickness and sections were mounted on 200-mesh copper grids. Sections were imaged at 120 kV using a FEI Tecnai 12 TEM outfitted with an AMT XR80C CCD Camera System, housed in the Facility for Electron Microscopy Research (FEMR) at McGill University. The sizes of pre-peroxisomes on mitochondria were measured with ImageJ (NIH).

For immuno-gold labelling, cells infected with Ad-Pex3–YFP or Ad-Pex16–YFP for 24 h were fixed in 5% PFA and 0.1% GA in PBS for 15 min at 37 °C. After washing with PBS, aldehydes were quenched with 50 mM glycine in PBS. Cells were permeabilized with 0.1% saponin and 5% BSA in PBS for 30 min at room temperature. Cells were incubated with anti GFP-antibody for 1 h at room termperature. After washing with 1% BSA in PBS, cells were incubated with 1.4 nm nanogold-conjugated goat anti-rabbit IgG for one hour at room temperature. After washing with PBS, cells were post-fixed with 1.6% GA in PBS for 10 min at room temperature. Cells were washed with water, then nanogold particles were enhanced using the HQ Silver Enhancement Kit (Nanoprobes) according to the manufacturer's instructions. Cells were stored in 1.6% GA in 0.1 M sodium cacodylate at 4 °C overnight and processed as for conventional TEM (described above).

Subcellular fractionation. Cells resuspended in ice-cold homogenization buffer (HB, 10 mM HEPES-KOH pH 7.4, 220 mM manitol, 70 mM sucrose, protease inhibitor cocktail) were homogenized with a 27-G needle (BD). Post-nuclear supernatants after centrifugation at 800*g* for 10 min were centrifuged at 2,300*g* for 10 min. Supernatants were further centrifuged at 23,000*g* for 15 min and at 100,000*g* for 1 h. After each centrifugation, pellets were resuspended in HB. Protein concentrations were measured by the Bradford method and analysed by immunoblotting.

Sub-organellular localization. Twenty-five micrograms of 2.3 K for mitochondrial or 23 K for peroxisomal fractions suspended in 40 μl of mitochondrial isolation buffer (MIB, 10 mM HEPES pH 7.4, 68 mM sucrose, 80 mM KCl, 0.5 mM EDTA, 2 mM $Mg(CH_3COO)_2$) containing varying amounts of trypsin (Sigma) were incubated on ice for 20 min. Digestion was terminated by adding soybean trypsin inhibitor (2.5 mg/ml, Sigma). For alkaline carbonate extraction, 50 μg of each fraction suspended in 50 μl of 0.1 M Na_2CO_3 pH 11.5 was incubated on ice for 30 min. Soluble and membrane fractions were separated by centrifugation at 200,000*g* for 15 min at 4 °C.

***In vitro* import assay.** Cell-free mitochondrial import assays were performed as previously described[34], with some modifications. In brief, Pex3– and Pex16–myc-His inserted into pCDNA3.1 myc-His (-) B (Invitrogen) were linearized by AgllI restriction enzyme (NEB) before *in vitro* transcription. Capped RNA was synthesized *in vitro* using T7 polymerase (Promega). For the co-translational import assay, synthesized RNA was incubated with rabbit reticulocyte lysate (RRL, Promega) and 14.4 μg of canine pancreas microsomes[35,36] for 30 min at 30 °C. Microsomes were collected by centrifugation at 100,000*g* for 15 min after washing with MIB twice. For post-translational import into isolated mitochondria, synthesized RNA was incubated with RRL for 30 min at 30 °C. Reaction products were incubated with 50 μg mitochondria isolated from mouse heart[34] in 50 μl reaction mix (10 mM HEPES pH 7.4, 110 mM Mannitol, 68 mM sucrose, 80 mM KCl, 0.5 mM EGTA, 2 mM $Mg(CH_3COO)_2$, 0.5 mM GTP, 2 mM K_2HPO_4, 1 mM ATP (K^+), 0.08 mM ADP, 5 mM sodium succinate) for 30 min at 30 °C. Mitochondria were washed with MIB twice and subjected to further analysis for suborganellular localization as described above or directly analysed by immunoblotting.

Immunoprecipitation for Pex3 ubiquitination. $Pex3^{mut}$ cells infected with Ad-GFP or Ad-Pex3–YFP for 10 h were further treated with or without 500 nM MG132 for 14 h. Cells were lysed with 0.1% SDS lysis buffer (50 mM Tris-HCl

pH 7.4, 150 mM NaCl, 5 mM EDTA, 0.1% SDS, 1% Triton-X 100, protease inhibitor cocktail and PhosStop). Soluble fractions were obtained by centrifugation at 20,000*g* for 20 min at 4 °C. Non-specific binding proteins were removed by rotating with protein-G sepharose (GE Healthcare) for 1 h at 4 °C. Lysates were subjected to immunoprecipitation using rabbit polyclonal anti-GFP antibodies (Invitrogen). Immmunoprecipitates were eluted by adding SDS–PAGE sample buffer and analysed by immunoblotting.

qRT–PCR. Total RNA was isolated from each cell using RNeasy kit (QIAGEN). qRT–PCR and data analysis were performed at IRIC Genomics Platform (University de Montreal). Primers are as follows: ACTB (endogenous control) (Fw: attggcaatgagcggttc, Rv: tgaaggtagtttcgtggatgc), GAPDH (endogenous control) (Fw: agccacatcgctcagacac, Rv: gcccaatacgaccaaatcc), Pex19 (Fw: gcaagtcggaggtagcaaga, Rv: ctttatcgaaatcatcaagagcac), Pex3 (Fw: aaccagaggacttgcaatatgac, Rv: tgctgcattaaggcctctct), Pex16 (Fw: aggtgtgggtgtgaagtgg, Rv: caggagcatccgcagtaca).

Statistical analysis. The means of each condition were calculated from three independent experiments, counting at least 30 cells per condition to generate enough power for statistical significance. *P* values for data comparison were calculated by Student's *t*-test. No statistical methods were used to predetermine sample size. The experiments were not randomized and the investigators were not blinded to allocation during experiments and outcome assessment.

Reproducibility. All data shown here have been reproduced at least three times by the authors.

Data availability. All data supporting the findings of this study are available within the paper and the supplementary information files.

30. Jeyaraju, D. V. *et al.* Phosphorylation and cleavage of presenilin-associated rhomboid-like protein (PARL) promotes changes in mitochondrial morphology. *Proc. Natl Acad. Sci. USA* **103,** 18562–18567 (2006).
31. Yao, J. & Shoubridge, E. A. Expression and functional analysis of SURF1 in Leigh syndrome patients with cytochrome c oxidase deficiency. *Hum. Mol. Genet.* **8,** 2541–2549 (1999).
32. Neuspiel, M., Zunino, R., Gangaraju, S., Rippstein, P. & McBride, H. Activated mitofusin 2 signals mitochondrial fusion, interferes with Bax activation, and reduces susceptibility to radical induced depolarization. *J. Biol. Chem.* **280,** 25060–25070 (2005).
33. Neuspiel, M. *et al.* Cargo-selected transport from the mitochondria to peroxisomes is mediated by vesicular carriers. *Curr. Biol.* **18,** 102–108 (2008).
34. McBride, H. M., Millar, D. G., Li, J. M. & Shore, G. C. A signal-anchor sequence selective for the mitochondrial outer membrane. *J. Cell Biol.* **119,** 1451–1457 (1992).
35. Walter, P. & Blobel, G. Preparation of microsomal membranes for cotranslational protein translocation. *Methods Enzymol.* **96,** 84–93 (1983).
36. Nguyen, M., Millar, D. G., Yong, V. W., Korsmeyer, S. J. & Shore, G. C. Targeting of Bcl-2 to the mitochondrial outer membrane by a COOH-terminal signal anchor sequence. *J. Biol. Chem.* **268,** 25265–25268 (1993).
37. McBride, H. M., Goping, I. S. & Shore, G. C. The human mitochondrial import receptor, hTom20p, prevents a cryptic matrix targeting sequence from gaining access to the protein translocation machinery. *J. Cell Biol.* **134,** 307–313 (1996).
38. Sugiura, A., McLelland, G. L., Fon, E. A. & McBride, H. M. A new pathway for mitochondrial quality control: mitochondrial-derived vesicles. *EMBO J.* **33,** 2142–2156 (2014). 10.15252/embj.201488104

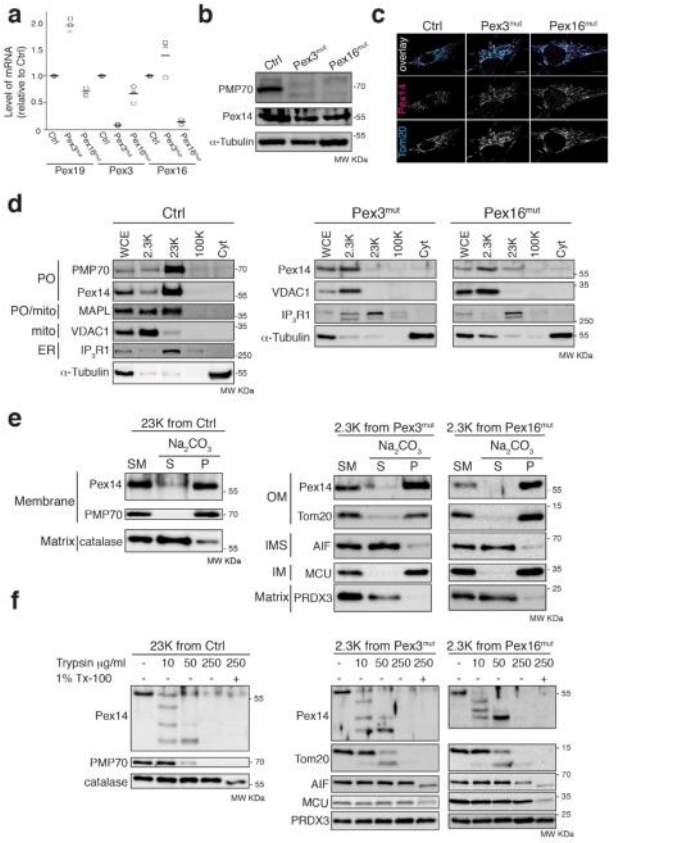

Extended Data Figure 1 | Characterization of cell lines used in this study. a, Levels of *PEX19*, *PEX3* and *PEX16* mRNA in each cell line were quantified by qRT–PCR. Data show mean ± s.e.m. of each mRNA normalized to control cells from three biological independent experiments. **b**, Levels of PMP70 and Pex14 protein were determined by immunoblotting analysis using the indicated antibodies. **c**, Control, Pex3^{mut} and Pex16^{mut} cells were subjected to immunfluorescence using the indicated antibodies. Representatives of captured images: Ctrl (16), Pex3^{mut} (51), Pex16^{mut} (98) shown. Scale bars, 10 μm. **d**, Subcellular fractionation of control and mutant cells. Isolation of whole-cell extracts (WCE), a 2.3K pellet enriched for mitochondria, a 23K pellet containing ER and peroxisomes, and a 100K pellet as a light membrane fraction showed clear separation of resident markers of these organelles. We analysed 7.5 μg of each fraction isolated from cells by immunoblotting using the indicated antibodies as organelle markers. 2.3K, 23K and 100K: precipitates after centrifugation at indicated speeds. Cyt: supernatants after centrifugation at 100,000*g*. **e**, **f**, The 23K fraction isolated from control cells or 2.3K fraction isolated from mutant cells were further separated into soluble (S) and membrane (P) fractions by alkaline carbonate extraction (**e**) or digested with trypsin at indicated concentrations (**f**). After the treatments, samples were analysed by immunoblotting using the indicated antibodies.

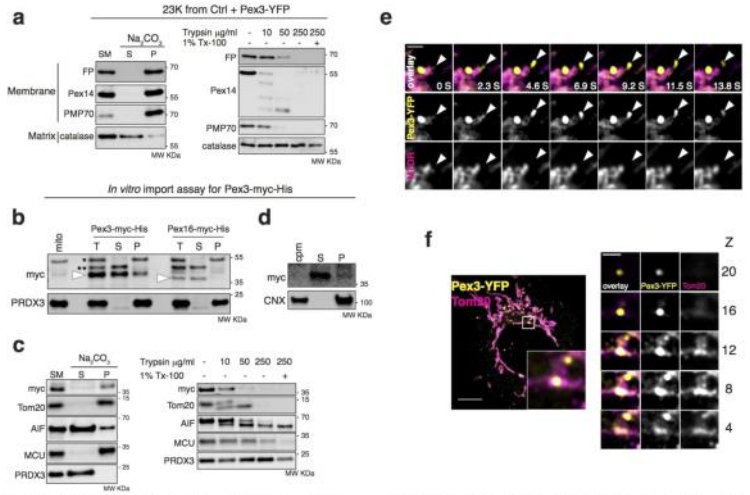

Extended Data Figure 2 | Pex3–YFP is inserted into mitochondrial outer membrane and assembles into mitochondria-derived pre-peroxisomal structures. a, Left, 23K fraction enriched for peroxisomes, isolated from control cells infected with Ad-Pex3–YFP for 1 day, was separated into soluble and membrane fractions by alkaline carbonate extraction. Internal controls for the efficiency of extraction are shown using antibodies detecting endogenous mitochondrial proteins. Right, protease sensitivity of each protein. Isolated peroxisomes were digested by trypsin at indicated concentrations in the absence or presence of 1% tritonX-100 to ensure full protease accessibility as control (right). After the treatments, samples were analysed by immunoblotting using the indicated antibodies. **b**, Pex3, but not Pex16, was imported efficiently into the mitochondrial outer membrane *in vitro*. *In vitro* translated Pex3 and Pex16 were incubated with mitochondria isolated from mouse heart[34,37]. Following the reaction, mitochondria were isolated by centrifugation (P), and the supernatants collected (S). The initial total reaction (T) was also loaded for comparison. Fractions were analysed by immunoblotting using the indicated antibodies. Arrowheads indicate Pex-myc-His. Single and double asterisks indicate nonspecific signals from mitochondria and rabbit reticulocyte lysate, respectively. **c**, Post-import fractionation of Pex3–YFP. Left, following the import reaction, membrane proteins were extracted using sodium carbonate and pelleted, with soluble proteins remaining in the supernatant. Right, protease protection experiment with increasing concentrations of trypsin and samples analysed by immunblotting, along with the indicated internal controls. Pex3–YFP is shown to be trypsin sensitive and alkali resistant, confirming its carbonate-resistant import into the mitochondrial outer membrane *in vitro*. **d**, Co-translational import of Pex3 into microsomes *in vitro*. Synthesized RNA was incubated with rabbit reticulocyte lysate and canine pancreas microsomes (cpm)[35]. Supernatants and pellets after centrifugation at 100,000g were analysed by immunoblotting using the indicated antibodies. In contrast to a previous study[18], but consistent with the primary mitochondrial localization of Pex3–YFP in Pex3^{mut} fibroblasts, Pex3 was very weakly detected in the microsome fraction following the import reaction. Calnexin (CNX) reveals the efficient isolation of microsomal membranes in the pellet fraction. **e**, Captured images from live cell imaging of Pex3^{mut} cells infected with Ad-Pex3–YFP for 1 day and stained with MitoTracker deep red (sVideo4). Arrowheads indicate Pex3–YFP-enriched structure budding from mitochondrion and lacking MitoTracker, distinguishing the release of Pex3–YFP-positive structure from normal mitochondrial fission. Representative of 47 movies is shown. Scale bar: 2 µm. **f**, *Z* series images of Pex3^{mut} cells infected with Ad-Pex3–YFP were acquired (21 sections, 0.1 µm per section). Left, stacked image. Numbers in right panels indicate *Z* sections of inset in left (all sections shown in Supplementary Video 6). Representative of 60 captured cells is presented. Scale bar: left, 10 µm; right, 2 µm.

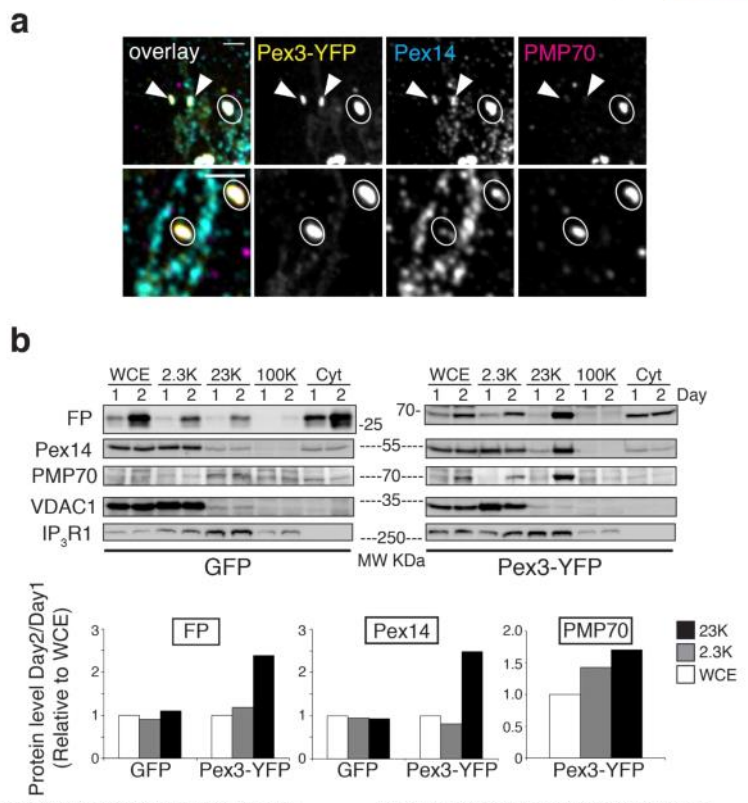

Extended Data Figure 3 | Endogenous Pex14 is sorted into mitochondrial pre-peroxisome with Pex3–YFP. a, PMP70 is rapidly incorporated into pre-peroxisomes. Pex3^{mut} cells infected with Ad-Pex3–YFP for 1 day were subjected to immunofluorescence using the indicated antibodies. Representatives of 50 captured cells are presented. Arrowheads, Pex3–YFP- and Pex14-positive but PMP70-negative pre-peroxisomes, defined as stage I. Circles, all positive structures. Scale bars: 2 μm. **b**, Pex3^{mut} cells infected with Ad-GFP or Ad-Pex3–YFP for 1 or 2 days were fractionated. Each fraction was loaded with 7.5 μg protein, and cellular levels of Pex3–YFP and PMP70 increased throughout the rescue. PMP70 is known to be degraded when peroxisomes are absent, and stabilized upon the generation of import-competent organelles. Quantification of Pex3–YFP, Pex14 and PMP70 in each fraction at each time point was normalized to the total expression in whole cell extracts (WCE). The graphs represent means from three independent experiments. Two days after infection, Pex3–YFP was enriched in the 23K peroxisomal fraction by more than twofold, and PMP70 levels were stabilized in the newly generated peroxisomes. Endogenous Pex14 was found in the mitochondrial fraction (2.3K) of both GFP and Pex3–YFP infected cells, and shifted into the peroxisomal fraction after 2 days of Pex3–YFP expression.

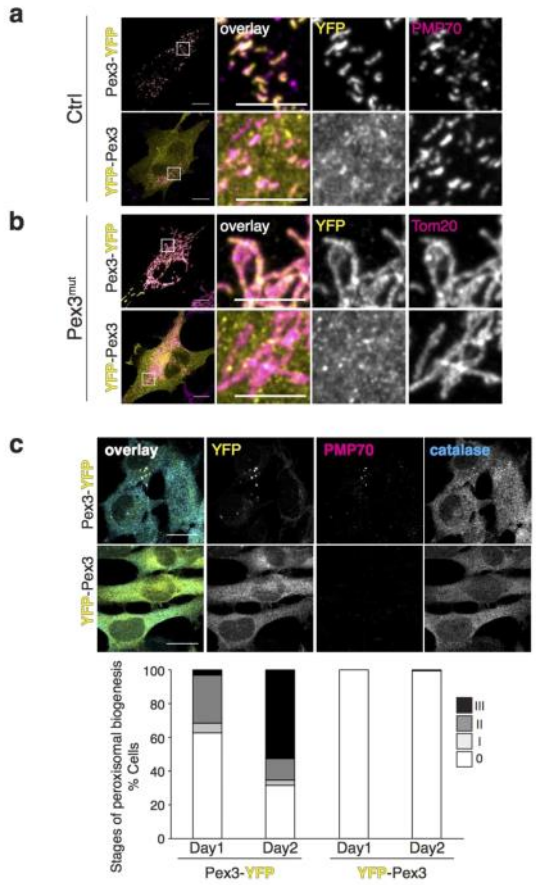

Extended Data Figure 4 | N-terminal YFP-tagged Pex3 fails to import into mitochondria and cannot rescue peroxisomal biogenesis in Pex3^{mut} cells. a, **b**, Control (**a**) or Pex3^{mut} cells (**b**) transfected with Pex3–YFP or YFP–Pex3 were subjected to immunofluorescence using the indicated antibodies. Representatives of captured cells: Ctrl + Pex3–YFP (12), Ctrl + YFP–Pex3 (27), Pex3^{mut} + Pex3–YFP (27), Pex3^{mut} + YFP–Pex3 (62) are presented. YFP–Pex3 inefficiently targets peroxisomes in control cells and mitochondria in Pex3^{mut} cells. Scale bars: low magnification, 10 μm; high magnification, 5 μm. **c**, Representatives of counted cells from 1 day after transfection are shown. The graph represents percentage of cells at each stage of *de novo* synthesis. Error bars show means from three biological replicates. Pex3–YFP: day 1 (52, 51, 51), day 2 (51, 53, 51); YFP–Pex3: day 1 (50, 50, 52), day 2 (50, 50, 51) cells were counted in each experiment. Scale bars: 20 μm

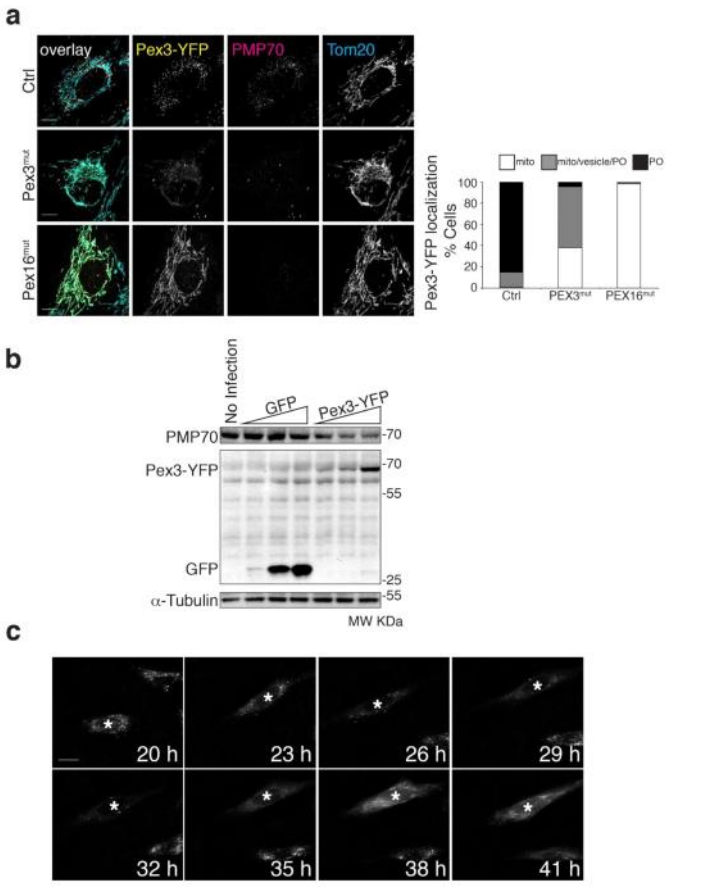

Extended Data Figure 5 | Pex3–YFP localization in the presence or absence of peroxisomes. a, Control, Pex3^{mut}, and Pex16^{mut} cells infected with Ad-Pex3–YFP for 1 day were subjected to immunofluorescence using the indicated antibodies. Representative of counted cells are presented. Quantification of the Pex3–YFP localization was performed from fixed confocal images. Error bars represent the mean from three biological independent experiments. Cells counted in each experiment: control (59, 81, 79), Pex3^{mut} (69, 62, 73), Pex16^{mut} (40, 45, 51). Scale bars: 10 μm. **b**, Control cells infected with varying amounts of Ad-GFP or Pex3–YFP were analysed by immunoblotting using indicated antibodies. **c**, Captured images from live cell imaging (Supplementary Video 7). Control cells were monitored for 2 days after infection with Ad-Pex3–YFP. Times indicate hours after infection. At 20 h, Pex3–YFP is exclusively peroxisomal within the cell (asterisk). The number of peroxisomes then steady declines between 20 and 32 h. Pex3–YFP expression is very low between 32 and 35 h, and slowly rises as it is imported into mitochondria, evident by 38–41 h. Representative of 30 movies is shown. Scale bar: 20 μm.

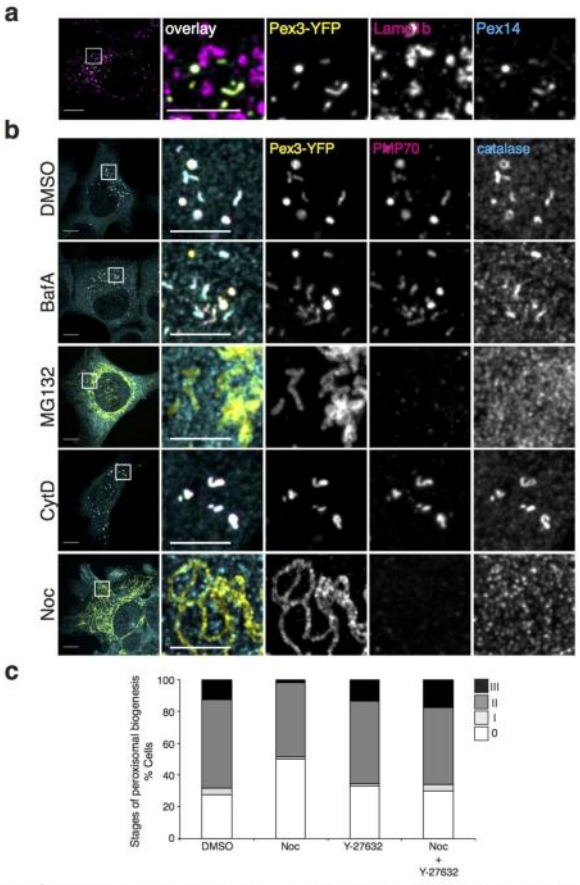

Extended Data Figure 6 | Pex3-mediated peroxisomal biogenesis is blocked upon addition of MG132 or nocodazole. a, Ad-Pex3–YFP did not colocalize with lysosomal markers within $Pex3^{mut}$ cells. Representative of 171 captured cells shown. Scale bars: low magnification, 10 μm; high magnification, 5 μm. **b**, Representative images of PMP70 and catalase staining shown in Fig. 3c. Scale bars: low magnification, 10 μm; high magnification, 5 μm. **c**, Ten hours after infection with Ad-Pex3–YFP, $Pex3^{mut}$ cells were incubated with 0.02% DMSO, 1.5 μM nocodazole or 5 μM Y-27632 for 14 h. Stages of *de novo* synthesis were classified and quantified using confocal imaging. The graphs represent mean from three biological replicates. Cells counted in each experiment: DMSO (50, 56, 51), Noc (50, 54, 51), Y-27632 (53, 51, 53), Noc + Y-27632 (51, 54, 51).

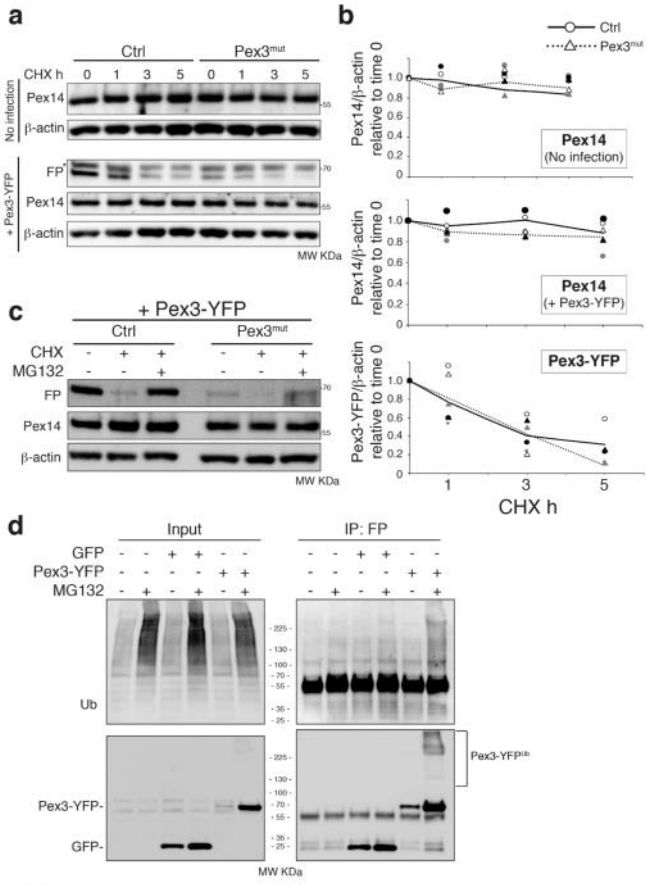

Extended Data Figure 7 | See next page for caption.

Extended Data Figure 7 | Pex3 is rapidly turned over from both mitochondrial and peroxisomal locations. a, **b**, Control and Pex3^{mut} cells infected with Ad-Pex3–YFP or not infected for 1 day were chased with 20 μg ml^{-1} cycloheximide (CHX) for indicated times. Protein levels were analysed by immunoblotting using the indicated antibodies and quantified by densitometric analysis. Line graphs and plots of different shapes represent mean and each value from three independent experiments. Pex14 levels were very stable over the 5-h period, but Pex3–YFP was rapidly depleted between 1 and 5 h. **c**, One day after infection, cells were incubated with 20 μg ml^{-1} CHX and 2 μM MG132 for 5 h. Protein levels were analysed by immunoblotting using the indicated antibodies. Asterisks, nonspecific bands. The data show that loss of Pex3–YFP upon cyclohexamide treatment is through proteasome-dependent degradation from both the peroxisomal location (in control human fibroblasts) and from mitochondria (in Pex3^{mut} cells). Note that total expression of Pex3–YFP in Pex3^{mut} cells is significantly lower than in control fibroblasts. **d**, Pex3^{mut} cells infected with Ad-Pex3–YFP for 1 day were treated under the indicated conditions and subjected to immunoprecipitation using anti-FP antibody. Input and immunoprecipitates were analysed by immunoblotting using the indicated antibodies. GFP, Ad-GFP; Pex3–YFP, Ad-Pex3–YFP; MG132, 500 nM for 14 h. The immunoprecipitation shown in the last lane reveals the accumulation of ubiquitin-conjugated forms of Pex3–YFP in the presence of MG132 (Pex3–YFP^{Ub}), indicating that a ubiquitin E3 ligase is required for the steady-state turnover of Pex3.

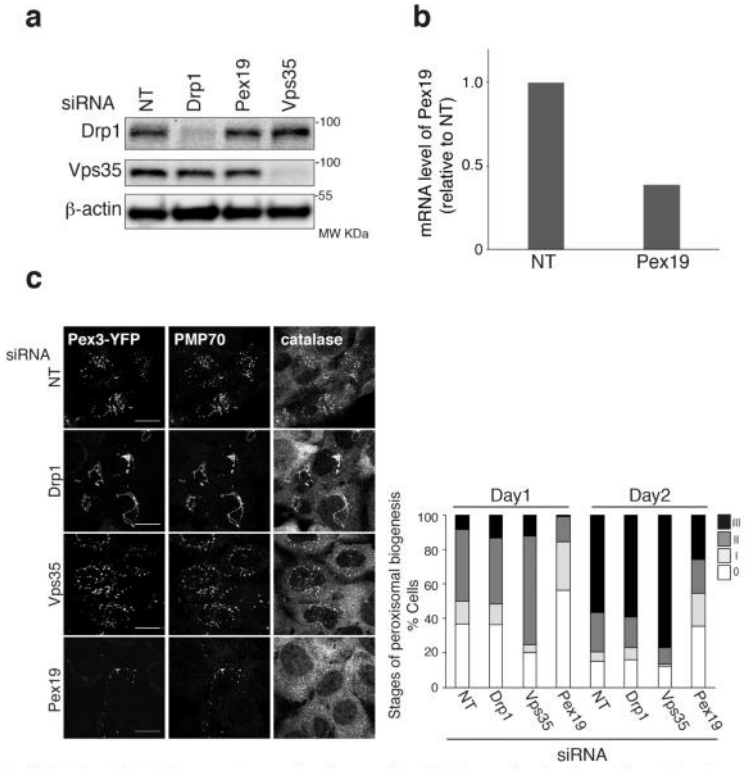

Extended Data Figure 8 | Pex3–YFP pre-peroxisomes are released from mitochondria by distinct machinery from mitochondrial fission and mitochondrial vesicular transport to peroxisomes. a, **b**, $Pex3^{mut}$ cells were silenced with siRNAs targeting Drp1, Vps35 or Pex19 for 3 days. Drp1 is a fission GTPase that is essential for mitochondrial and peroxisomal membranes[23]. Mitochondrial vesicle formation occurs in a manner independent of Drp1 (ref. 38), and this experiment was to test whether exit of Pex3–YFP from mitochondria in vesicular profiles requires this GTPase. Vps35 is a subunit of the retromer complex, which plays a critical role in the steady-state transport of mitochondrial vesicles to peroxisomes[23]. Pex19 is the cytosolic chaperone that binds and delivers peroxisomal membrane proteins to Pex3–Pex16 for insertion[9,17]. This experiment was to test whether Pex19 was required for Pex3 import into mitochondria. Knockdown efficiency was determined by immunoblotting using the indicated antibodies (**a**) or qRT–PCR (**b**). **c**, $Pex3^{mut}$ cells silenced (as indicated) for 3 days were infected with Ad–Pex3–YFP. One or two days after infection, cells were subjected to immunofluorescence using the indicated antibodies. Left panels, representatives of counted cells at day 2. The graph represents the percentage of cells at each stage. Error bars show mean from three biologically independent experiments. Cells counted in each experiment: control (N): day 1 (55, 86, 55), day 2 (90, 90, 70); Drp1: day 1 (56, 63, 65), day 2 (103, 103, 87); Vps35: day 1 (59, 81, 77), day 2 (83, 83, 88); Pex19: day 1 (39, 66, 68), day 2 (61, 61, 59). Although Drp1 was essential for peroxisomal division, its loss did not alter peroxisome biogenesis or import competence. Loss of Vps35 appeared to enhance the rate of peroxisomal biogenesis, but Vps35 was clearly not required for Pex3–YFP-mediated rescue. Loss of Pex19 did not alter Pex3–YFP insertion into mitochondria or the generation of stage I pre-peroxisomes. These peroxisomes did not mature, suggesting that the roughly 60% loss of Pex19 was functionally sufficient to completely block peroxisomal protein import. Scale bars: 20 μm.

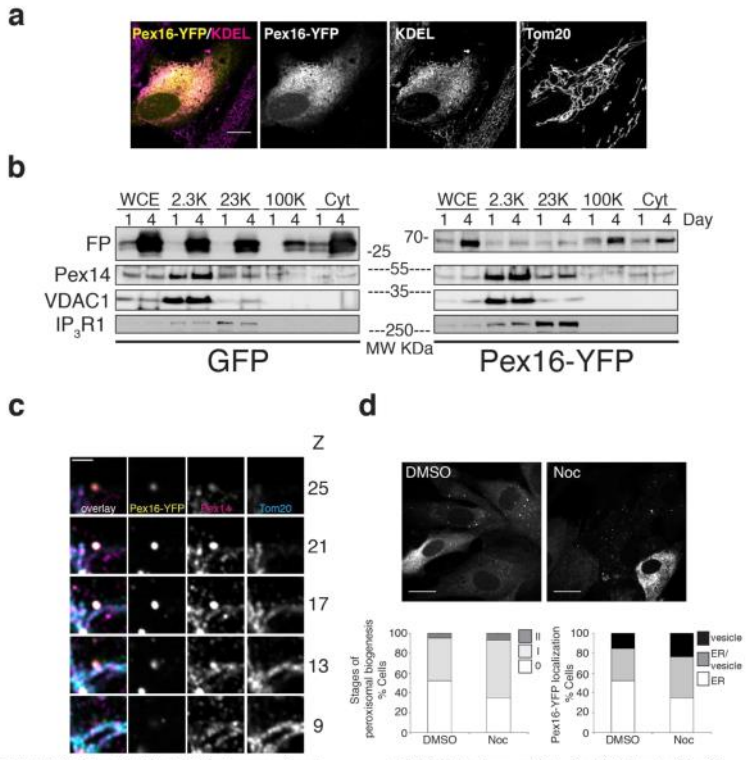

Extended Data Figure 9 | Ad-Pex16–YFP restores peroxisomal biogenesis in human fibroblasts lacking Pex16 from a patient with Zellweger. a, Pex16^{mut} cells infected with Ad-Pex16–YFP for 1 day were subjected to immunofluorescence using anti-Tom20 (mitochondria) and anti-KDEL (ER) antibodies. A representative of 34 captured cells is presented. Scale bar: 10 μm. The ER is primarily sheet-like rather than reticular within Pex16^{mut} cells, and Pex16–YFP primarily follows that pattern, which is completely distinct from the mitochondrial staining. **b**, Each fraction isolated from Pex16^{mut} cells infected with Ad-GFP or Ad-Pex16–YFP for 1 or 4 days was analysed by immunoblotting. **c**, Pex16-positive vesicular profiles localize to mitochondrial tubules where they acquire endogenous Pex14. *Z* series images of Pex16^{mut} cells infected with Ad-Pex16–YFP and immunostained with anti-Pex14 and anti-Tom20 (32 sections, 0.1 μm per section). The numbers represent images at indicated *Z* (all sections shown in Supplementary Video 8). Representatives of 31 captured cells are presented. Scale bar: 2 μm. **d**, Pex16–YFP transition to stage I is unaffected by nocodazole. Ten hours after infection with Ad-Pex16–YFP, Pex16^{mut} cells were incubated with 0.02% DMSO or 1.5 μM nocodazole for 14 h. Representatives of counted cells are presented. Stages of *de novo* synthesis (left) or localization of Pex16–YFP (right) were determined under the confocal microscope. Error bars show mean from three biologically independent experiments. Cells counted in each experiment: DMSO (56, 51, 52), Noc (54, 53, 51). Representative images of Pex16–YFP are shown. Scale bars: 20 μm.

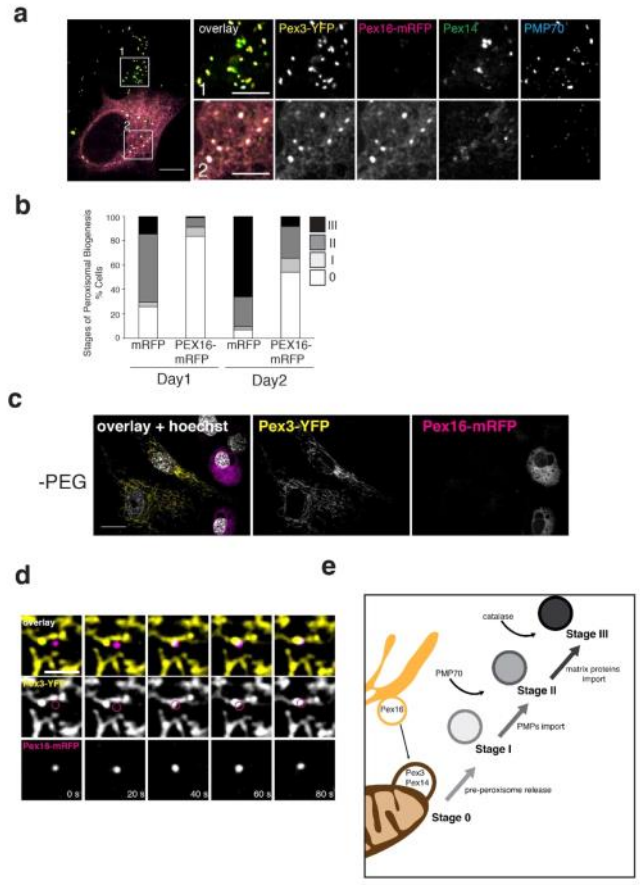

Extended Data Figure 10 | See next page for caption.

Extended Data Figure 10 | Peroxisome assembly requires both mitochondrial and ER-derived pre-peroxisomes. a, One day after transfection with Pex16–mRFP, Pex3^{mut} cells were infected with Ad-Pex3–YFP for further 1 day. Cells were subjected to immunofluorescence using anti-Pex14 and anti-PMP70 antibodies. Insets in left images are shown in right panels. Representatives of 32 captured cells are presented. Scale bars: low magnification, 20 μm; high magnification, 5 μm. **b**. Pex3^{mut} cells were transfected with mRFP or Pex16–mRFP for 24 h before infection with Ad-Pex3–YFP. Cells were subjected to immunofluorescence 1 or 2 days after Pex3–YFP infection. The graph represents the percentage of cells at each stage of *de novo* synthesis as defined in Fig. 1a. The graph represents mean from three biological replicates. Cells counted in each experiment: mRFP: day 1 (58, 49, 68), day 2 (47, 73, 61); Pex16–mRFP: day 1 (37, 52, 55), day 2 (54, 50, 50). **c**, Pex16^{mut} cells expressing Pex3–YFP and Pex3^{mut} cells expressing Pex16–mRFP were co-plated in a glass-bottom cell culture dish. A representative of 17 images captured before addition of PEG is presented. Scale bar: 20 μm. **d**, Pex16^{mut} cells expressing Pex3–YFP and Pex3^{mut} cells expressing Pex16–mRFP were fused by PEG. Captured images are from live-cell imaging 3 h after PEG-mediated whole-cell fusion (Supplementary Video 10). Circles highlight Pex16 vesicle structures that fuse with Pex3 vesicle structures. Scale bar: 4 μm. **e**, Model of peroxisomal biogenesis in mammalian system. Pex16-containing pre-peroxisomes emerge from the ER. They then fuse with Pex3–Pex14 pre-peroxisomes at the mitochondrial surface, thereby generating an import-competent, functional peroxisome that proliferates through growth and division.